EXPLORE
Newsletter for the
Association of Applied Geochemists
www.appliedgeochemists.org

NUMBER 201 December 2023

Inverting the missing SiO_2 and LOI contents in the North American Soil Geochemical Landscapes datasets

Patrice de Caritat
Geoscience Australia, GPO Box 378, Canberra, ACT 2601, Australia (Patrice.deCaritat@gmail.com)

Eric C. Grunsky
Department of Earth & Environmental Sciences, University of Waterloo, Waterloo, ON N2L 3G1, Canada

David B. Smith
International Union of Geological Sciences Commission on Global Geochemical Baselines, Wheat Ridge, CO 80033, USA
https://doi.org/10.70499/XUYZ7021

INTRODUCTION

Rock, sediment and soil chemical and mineralogical compositions are fundamental to the discipline of geochemistry, as they affect or even control their bulk properties. Many geological materials on Earth contain silicates, phyllosilicates, and, perhaps less commonly, carbonates (e.g. Finkl 1981; Schaetzl and Anderson 2007; Deer et al. 2013). These mineral groups impact the materials' geochemical compositions in terms of SiO_2, H_2O and CO_2 concentrations (among others).

X-ray fluorescence (XRF) is a traditional analytical method used to obtain total concentration analyses, which are agnostic of the mineral host, element speciation or oxidation state. Major elements (> 0.1 weight percent (wt%) abundance) are typically reported as a suite of oxides (i.e. Al_2O_3, CaO). This suite of oxides is either directly obtained from XRF or converted from elemental data such as acquired by Inductively Coupled Plasma-Atomic Emission Spectroscopy (ICP-AES) or -Mass Spectrometry (ICP-MS) methods. The latter ICP methods do not report SiO_2, H_2O or CO_2 because of the sample digestion requirement.

The gravimetric determination of loss-on-ignition (LOI), obtained by heating the sample to a set temperature and measuring the mass loss relative to the starting sample (at standardized temperature, pressure and humidity), often complements the XRF or ICP analyses. LOI has several components, including adsorbed water (H_2O; e.g. interlayer water in clay minerals), combined H_2O (e.g. hydrated minerals and labile hydroxyl-compounds), carbon dioxide (CO_2; e.g. from carbonates and organic matter), and volatile elements (e.g. Hg).

One advantage of reporting the major components of a geological sample as oxides is that their sum, when complemented by LOI and trace elements (TEs), should add up to 100 wt%. Any discrepancy represents components not analyzed for and/or uncertainty. Having a complete sample analysis, or at least as complete as practically possible, is important to give confidence that the sample is well characterized, which implies that the composition is closed or full and not a subcomposition (i.e. no component is unaccounted for). This has implications in subsequent data analytics, including in the development and application of Compositional Data Analysis (CoDA) methods (e.g. Chayes 1960; Aitchison 1986; Scealy et al. 2015).

Another benefit of a complete sample analysis is the direct relationship between the geochemical and mineralogical compositions, via the knowledge (or modeling) of the minerals' stoichiometric compositions. Deriving the most plausible mineralogy from geochemistry is a non-unique inversion problem known as 'normative analysis' (e.g. Caritat et al. 1994; Aldis et al. 2023). It is a useful way to ensure that chemistry and mineralogy of a sample are consistent with one another.

THE NORTH AMERICAN SOIL GEOCHEMICAL LANDSCAPES PROJECT

The North American Soil Geochemical Landscapes (NASGL) project is a recent continental-scale geochemical survey of the conterminous United States of America (Smith et al. 2013, 2014, 2019; see Smith 2022 for a project review). Soils were sampled from three levels (0–5 cm depth, A horizon and C horizon) at 4857 sites, and their <2 mm fractions were analyzed for 45 major and trace element concentrations by methods yielding 'total or near-total' elemental content (mostly ICP-AES or ICP-MS after a four-acid — hydrochloric, nitric, hydrofluoric, and perchloric acids — digestion of the milled samples at 125° to 150°C; see Smith et al. 2013 for more detail). The chemical elements reported were Ag, Al, As, Ba, Be, Bi, C, Ca, Cd, Ce, Co, Cr, Cs, Cu, Fe, Ga, Hg, In, K, La, Li, Mg, Mn, Mo, Na, Nb, Ni, P, Pb, Rb, S, Sb, Sc, Se, Sn, Sr, Te, Th, Ti, Tl, U, V, W, Y, and Zn. Note that neither Si nor LOI were included in the contracted analytical package. As ICP-based analytical techniques cannot quantify O and H present (in fact, abundant) in most if not all geological samples, the sum of all its analytes (Al, …, Zn) falls well short of the ideal, complete composition of one million parts per million (ppm). Indeed in the NASGL C horizon dataset, used herein to illustrate our method, the sum of all ICP analytes ranges from 1134 to 390,740 (average 144,869) ppm.

The NASGL project also analyzed and quantified mineralogy in those samples. The minerals quantified were quartz, K-feldspars, plagioclases, (total feldspars), 14 Å clays (i.e. smectite), 10 Å clays (i.e. illite), kaolinite, (total clays), gibbsite,

continued on page 5

Inverting the missing SiO_2 and LOI contents ...

continued from page 1

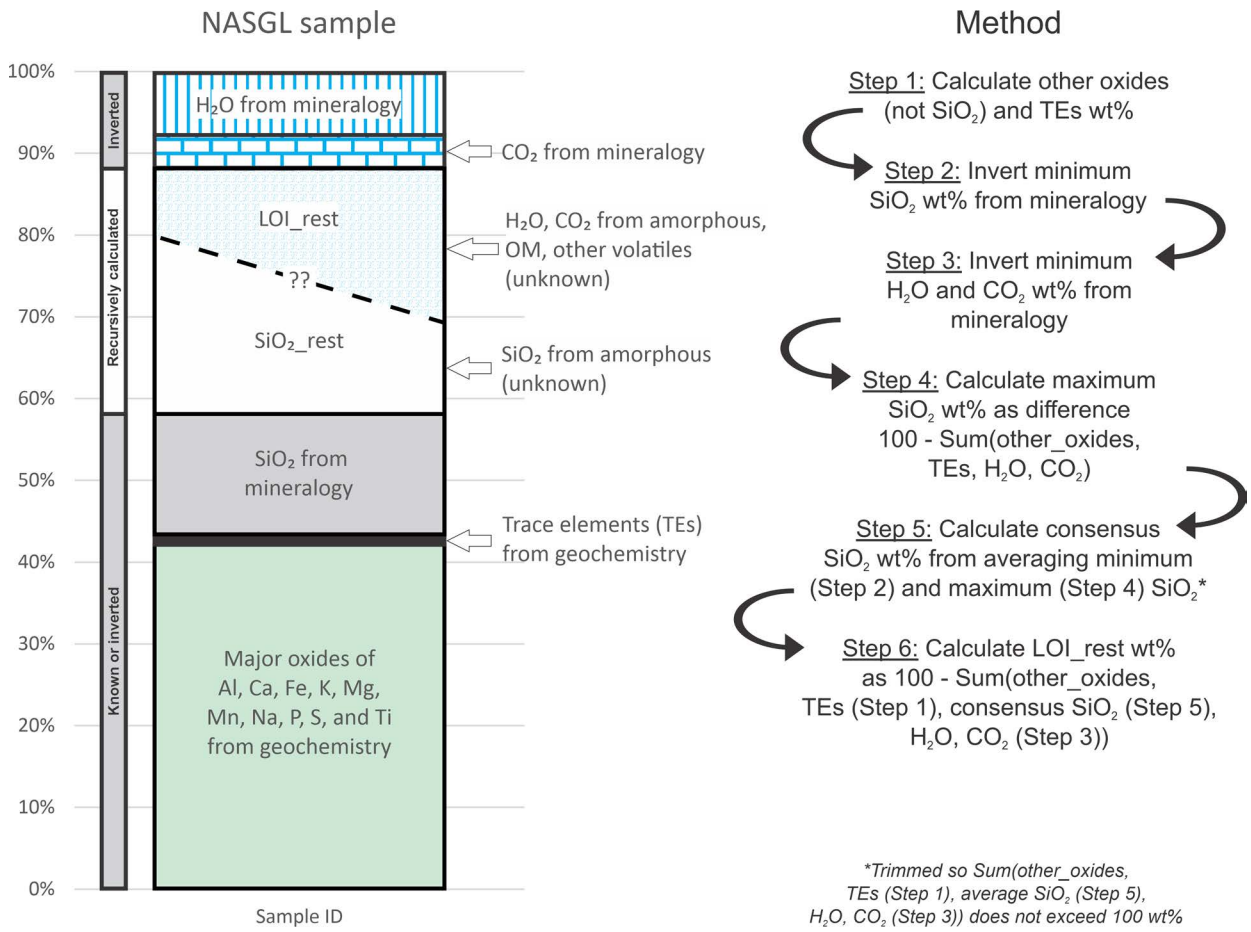

Fig 1. Conceptual diagram of an incomplete soil analysis and workflow of the SiO_2 and LOI recursive inversion estimation methodology developed herein using geochemistry and mineralogy.

calcite, dolomite, aragonite, (total carbonates), analcime, heulandite, (total zeolites), gypsum, talc, hornblende, serpentine, hematite, goethite, pyroxene, pyrite, other, and amorphous (phases in parenthesis are summations of other minerals). The amorphous phase typically consists of material that is poorly diffracting; this will generally include clay minerals, various forms of micro-quartz, Fe-, Mn- and Al-oxyhydroxides, organic matter, volcanic glass, etc. (e.g. Tan et al. 1970; Smith et al. 2018; Tsukimura et al. 2021). Minerals were identified by X-Ray Diffraction (XRD) and quantified using a Rietveld refinement method (Smith et al. 2013). Unlike the geochemical data, the XRD data are 'complete' in the sense that they do add up to 100 wt% (range 99.6 to 100.2, average 100.03, wt% for the C horizon). The present contribution develops and tests a method for estimating the missing, yet crucial, Si/SiO_2 and LOI concentrations.

INVERTING SiO_2 AND LOI FROM GEOCHEMISTRY AND MINERALOGY

As the NASGL project did not use XRF analysis, we first need to convert the 10 reported major elements (Al, Ca, Fe, K, Mg, Mn, Na, P, S, and Ti) into oxides and unify units to wt%. These oxides are hereafter referred to as 'other_oxides' to emphasize that they do not include SiO_2. The proposed method for estimating the missing SiO_2, which draws upon both the geochemical and the mineralogical analyses of the NASGL samples, is described below and the workflow is illustrated in Figure 1. A worked example is provided as a Microsoft Excel spreadsheet (https://doi.org/10.5281/zenodo.8191288).

Initially, two estimates for SiO_2 are calculated by inverting mineralogical information; neither is ideal, as the first is likely to give a minimum, and the second a maximum value for SiO_2. Next, a 'consensus' SiO_2 concentration is obtained recursively from the two aforementioned estimates. Finally, the LOI is calculated to obtain a closed full composition at 100 wt%. The detailed steps are described below.

Step 1: Data preparation. The geochemical and mineralogical data for soils of the conterminous United States (A and C horizon datasets) were downloaded from https://mrdata.usgs.gov/ds-801/. Samples (rows) that had either incomplete or missing geochemical or mineralogical quantification (e.g. insufficient sample material) were removed. Analytes (columns) with excessive censored values (below detection/reportable limit) were removed (e.g., Ag, Cs, Te; Grunsky et al. 2018). Concentration units were unified (ppm) and censored data were imputed using the zCompositions package (lrEM function) in the R computing environment (Palarea-Albaladejo et al. 2014). Note that the imputation step is not critical to the present estimation workflow and other ways of handling cen-

continued on page 7

Inverting the missing SiO_2 and LOI contents ...

continued from page 5

sored data may be applied. After imputation, the major elements were converted to oxides and all analytes were expressed as wt%.

Step 2: Inverting 'normative' SiO_2 due to silicate minerals. The **'normative' SiO_2** is the amount of SiO_2 each sample must contain to be consistent with its mineralogy (technically this is a reverse normative or inversion approach). This 'normative' SiO_2 calculates and sums the contributions in SiO_2 of each Si-bearing mineral (silicate), for example, **1 * quartz + 0.6476 * K-feldspar + … + AVERAGE (0.4830,0.5985,0.5549,0.5173) * pyroxene**. The multipliers are the proportions of the relevant oxide (e.g. SiO_2) in each mineral (e.g. K-feldspar above), and were sourced from https://webmineral.com. Where more than one end-member mineral exists for a group (e.g. a solid-solution), the average of the (most common) end-members is used (e.g. pyroxene above). This first estimate of SiO_2 does not consider the mineral phases 'other' and 'amorphous'. Amorphous has a median abundance of 17.5 wt% and a maximum of 95.2 wt% in the NASGL C horizon dataset. It is likely to contain forms of microcrystalline silica, such as opal-A; e.g., Achilles et al. 2018), and therefore the 'normative' SiO_2 calculated here could, and most likely does, underestimate the real SiO_2 concentration.

Step 3: Inverting LOI due to hydrate and carbonate minerals. The **'normative' H_2O** and **'normative' CO_2** components of LOI in each sample were calculated to be consistent with the mineralogy (e.g. amounts of gypsum and calcite). This is done in a similar way as described above, but applied to all O- and H-bearing (hydrate) minerals and all C-bearing (carbonate) minerals, respectively. As for SiO_2, the 'normative' H_2O and CO_2 contents of the amorphous phase are not known and likely important (e.g. Achilles et al. 2018). Thus this method could, and most likely does, underestimate the real LOI concentration.

Step 4: Calculating a second estimate for SiO_2. A second SiO_2 estimate is calculated by the difference **100 wt% - Sum(other_oxides, TEs, 'normative' H_2O, 'normative' CO_2)**. It could, and most likely does, overestimate the real SiO_2 concentration because LOI is almost certainly underestimated (see above). Note that in some instances, the first estimate of SiO_2 is larger than the second, which we interpret to result either from uncertainty in the mineralogical quantification (amounts of silicate, hydrate and carbonate minerals are not consistent with the geochemistry), or from an overestimation of 'normative' H_2O ('normative' CO_2 being well constrained by carbonate minerals).

Step 5: Recursively estimating a 'consensus' SiO_2. A **'consensus' SiO_2** is then calculated recursively by first taking the average of the above two SiO_2 estimates. For some samples, this SiO_2 estimate results in the **Sum(all_oxides, TEs, 'normative' H_2O, 'normative' CO_2)**, where all_oxides include the 'consensus' SiO_2 determined at Step 4, to exceed 100 wt%; in these cases, the SiO_2 estimate is trimmed so that this sum is 100 wt%.

Step 6: Calculating total LOI. Finally, the **LOI_rest**, that is volatiles others than the 'normative' H_2O and 'nor-

continued on page 9

Note: *This EXPLORE article has been extracted from the original EXPLORE Newsletter. Therefore, page numbers may not be continuous and any advertisement has been masked.*

Inverting the missing SiO_2 and LOI contents ...

continued from page 7

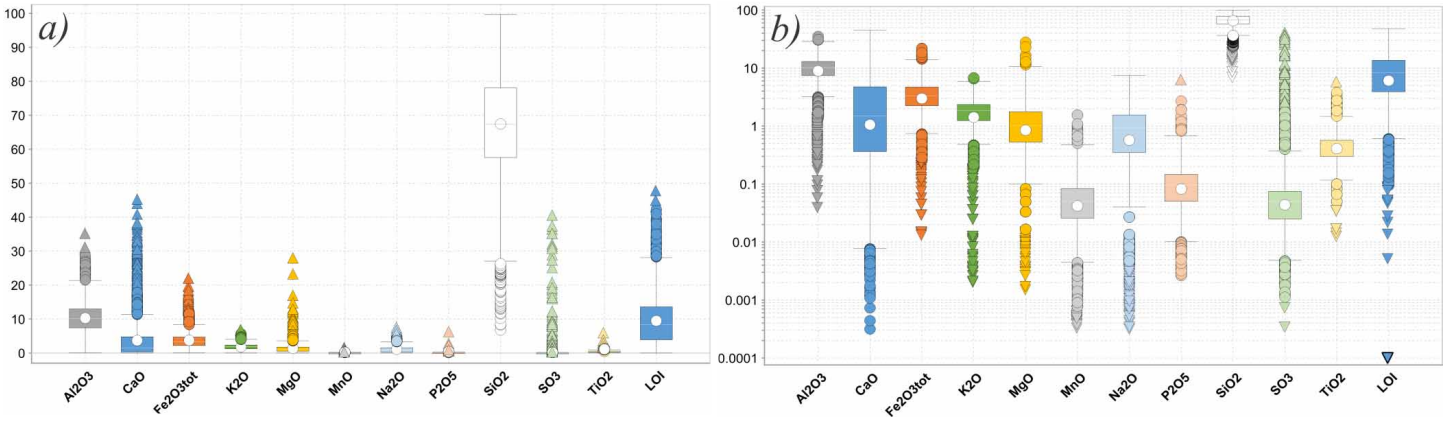

Fig. 2. Tukey boxplots for the major oxides (wt%) in the C horizon samples from the NASGL project (source: Smith et al. 2013), including SiO_2 and LOI estimated by the method described herein, with a linear (a) and log ordinate scale (b). Each box spans the 25th to 75th percentile (a.k.a. the inter-quartile range, IQR), the median is represented by a white/grey line inside the box, the mean by a white dot, the whiskers by T-shaped bars extending 1.5 x IQR away from the box, the inner outliers (up to 3 x IQR away from the box) by circles, and the outer outliers (more than 3 x IQR away from the box) by triangles.

mative' CO_2 calculated at Step 3 above, are calculated as the difference 1**00 wt% - Sum(all_oxides, TEs, 'normative' H_2O, 'normative' CO_2)**. This LOI_rest is likely to comprise H_2O and CO_2 in the amorphous phase as well as any other volatiles not specifically accounted for above. From here, total LOI or LOI_{tot} is calculated as **Sum('normative' H_2O, 'normative' CO_2, LOI_rest)**. Note that in a few cases where LOI_{tot} is zero it is replaced by 0.0001 wt% to allow log-transformation.

RESULTS AND DISCUSSION

Distributions of the SiO_2 and LOI estimates

The resultant final estimates for SiO_2 in the C horizon samples from the NASGL project have a distribution as represented in the Tukey boxplots (Tukey 1977) of Figure 2, which seem reasonable compared to the distribution of the other oxides. SiO_2 is clearly the most abundant major oxide in the NASGL soils, as is both expected and consistent with other regions (e.g. Australia, see Caritat and Cooper 2011a). The distribution of LOI is also illustrated in Figure 2. Table 1 summarizes the statistics of the estimated SiO_2 and LOI concentrations derived herein for both the A and C horizons.

Application to Selected NASGL Samples

Figure 3 shows the major oxide, including the SiO_2 estimated as described above, TEs, 'normative' H_2O, 'normative' CO_2, and LOI_rest of five selected samples from the NASGL C horizon dataset. Those samples were deliberately chosen to span the range of soil compositions in the dataset: sample from Site 7327 (California) is an Al-rich sample, 972 (Texas) is Ca-rich, 444 (Maryland) is Fe-rich, 12779 (Colorado) is K-rich, and 3808 (Florida) is Si-rich. Without the estimates for SiO_2 and LOI (and its components), only between 0.2 (3808) and 54 wt% (972) of those samples would be geochemically characterized; the rest would be unknown. This unknown 'gap' is shown by the present estimation technique to com-

Table 1. Summary statistics (count, minimum, median, average, maximum and standard deviation, in wt%) for the SiO_2 and LOI estimates in the A and C horizon samples from the NASGL project.

Variable	Count	Min	Med	Ave	Max	SD
SiO_2-A horizon	4800	7.25	72.02	72.07	99.8	13.96
SiO_2-C horizon	4669	6.78	67.37	67.44	99.63	15.18
LOI-A horizon	4800	0.0001	8.2	8.99	44.87	6.57
LOI-C horizon	4669	0.0001	8.36	9.48	47.57	7.02

continued on page 10

Inverting the missing SiO_2 and LOI contents ...

continued from page 9

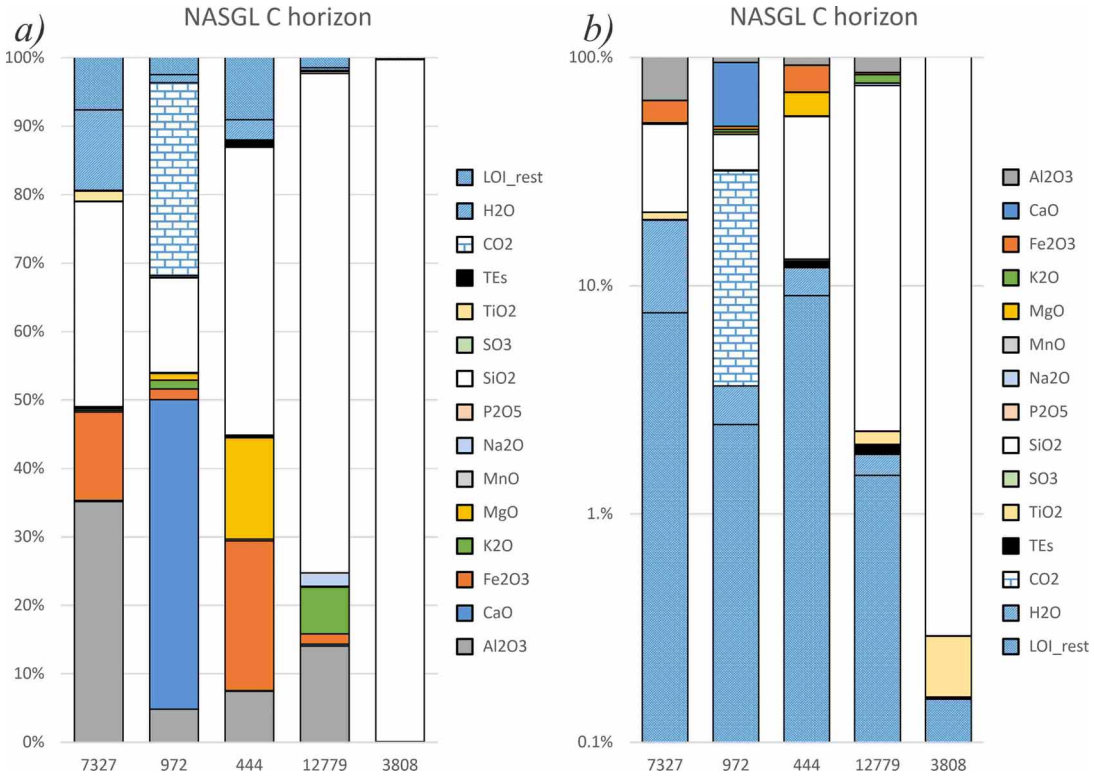

Fig. 3. Bar graphs showing the composition of five selected C horizon samples from the NASGL project (source: Smith et al. 2013) in terms of major oxides (wt%), including SiO_2 (white) and LOI (white with blue patterns) estimated by the method described herein, and trace elements (TEs). Components are shown in conventional order with a linear scale (a) and on a log scale in reverse order to emphasize the less abundant components (b).

prise widely varying proportions of SiO_2 (from silicates), H_2O (mainly from silicates), CO_2 (from carbonates), and other volatile phases (from the amorphous phase and possibly other volatile components). It is thus important to provide estimates for each sample that honor the known mineralogical characteristics rather than apply a one-size-fits-all estimation of these parameters.

Application to Selected NASGL Samples

Figure 3 shows the major oxide, including the SiO_2 estimated as described above, TEs, 'normative' H_2O, 'normative' CO_2, and LOI_rest of five selected samples from the NASGL C horizon dataset. Those samples were deliberately chosen to span the range of soil compositions in the dataset: sample from Site 7327 (California) is an Al-rich sample, 972 (Texas) is Ca-rich, 444 (Maryland) is Fe-rich, 12779 (Colorado) is K-rich, and 3808 (Florida) is Si-rich. Without the estimates for SiO_2 and LOI (and its components), only between 0.2 (3808) and 54 wt% (972) of those samples would be geochemically characterized; the rest would be unknown. This unknown 'gap' is shown by the present estimation technique to comprise widely varying proportions of SiO_2 (from silicates), H_2O (mainly from silicates), CO_2 (from carbonates), and other volatile phases (from the amorphous phase and possibly other volatile components). It is thus important to provide estimates for each sample that honor the known mineralogical characteristics rather than apply a one-size-fits-all estimation of these parameters.

For instance, sample 7327 contains significant clay minerals (40.5 wt% kaolinite) and thus has not only elevated Al_2O_3, but also elevated SiO_2 and LOI (H_2O) concentrations. Sample 972 contains significant carbonates (64.1 wt% calcite) as reflected not only by the elevated CaO, but also CO_2 concentrations. Sample 444 comprises significant amorphous

continued on page 11

Inverting the missing SiO_2 and LOI contents ...

continued from page 10

material (41 wt%) as well as notable clay (24.2 wt% of combined 14 Å clay and kaolinite), pyroxene, talc and hematite contents, imparting significant Fe_2O_{3tot}, MgO, moderate SiO_2 and relatively low LOI concentrations. Sample 12779 contains 60 wt% combined K-feldspar and plagioclase and some 10 Å clay, translating into a SiO_2-, Al_2O_3- and K_2O-rich geochemical makeup. Finally, sample 3808 contains 98.5 wt% quartz and 1.5 wt% K-feldspar, giving a geochemical composition overwhelmed by SiO_2 (estimated at 99.6 wt%); it probably also contains trace amounts of anatase or other Ti-bearing phase(s), undetected by the XRD method applied, to account for (some of) the 0.13 wt% TiO_2 reported geochemically.

Spatial Distributions of the SiO_2 in NASGL C Horizon

A map of the distributions of estimated SiO_2 concentrations in the NASGL C horizon is shown in Figure 4. The data are classified into ten quantile (decile) classes and coloured as per the mapping convention of Smith et al. (2014, 2019). The distribution shows strong similarities with the backdrop quartz distribution maps in the C horizon (Figure 141 in Smith et al. 2014), reflecting a dominant mineralogical control on the SiO_2 concentrations.

Validation and Uncertainty

Validation of the proposed method to estimate the missing SiO_2 and LOI data was performed in two different ways. The first was to apply the recursive inversion workflow to a dataset from Australia (Caritat et al. 2023) that includes both XRF (including SiO_2) and XRD data, and compare measured vs predicted SiO_2 concentrations (which gave $R^2 = 0.91$). The second was to iden-

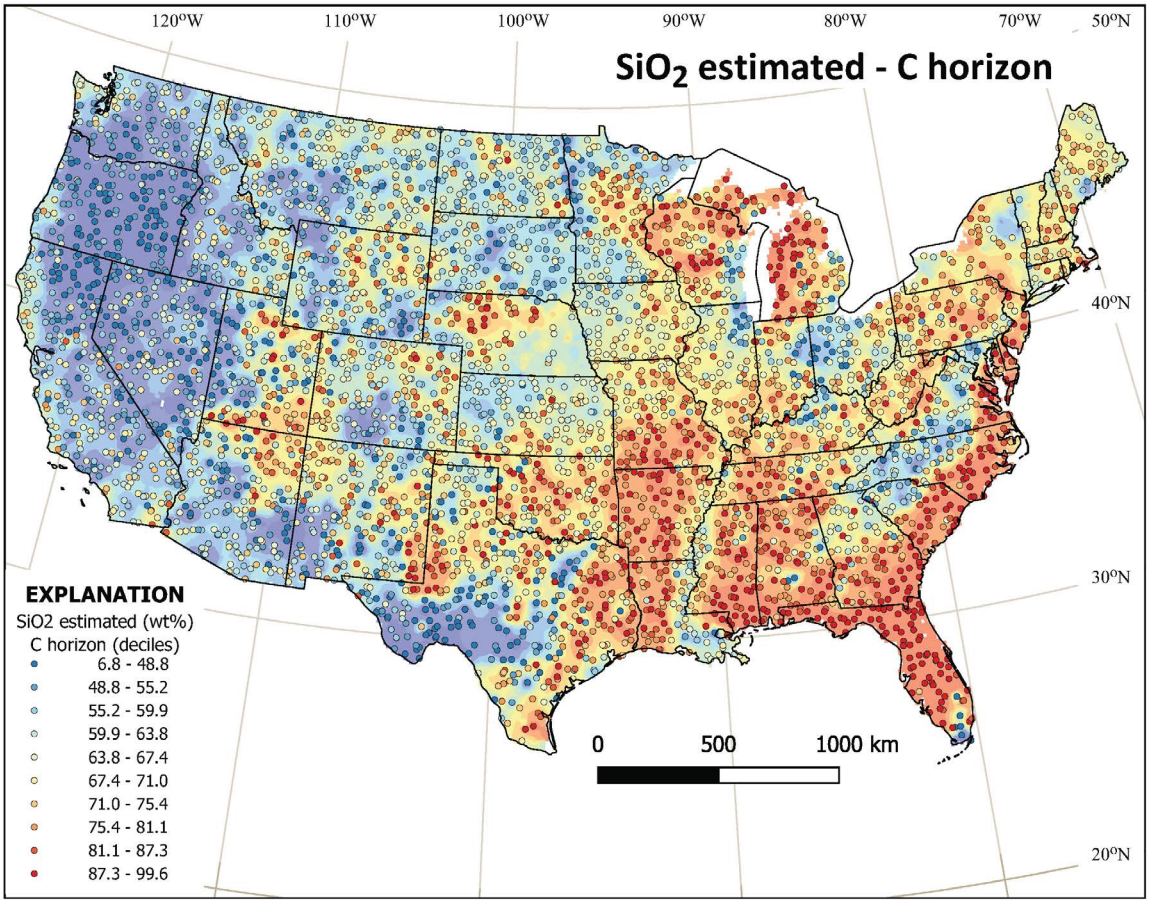

Fig. 4. Spatial distribution of the SiO_2 concentrations estimated herein for the C horizon of the NASGL samples across the USA. The symbols are classified and colored as per Smith et al. (2014), and overlain on the quartz distribution interpolated map (Figure 141 in Smith et al. 2014).

continued on page 12

Inverting the missing SiO_2 and LOI contents ...

continued from page 11

tify the closest NASGL samples to the 400 samples previously published Shacklette and Boerngen (1984) from the USA regolith geochemistry dataset (https://mrdata.usgs.gov/ussoils/) with measured SiO_2, and compare (1) the pairs of geographically 'adjacent' SiO_2 values (which gave $R^2 = 0.79$), and (2) the cumulative distribution functions of both SiO_2 values (measured by Shacklette and Boerngen and estimated from NASGL) by applying a Kolmogorov-Smirnov (K-S) test of distribution similarity (Kolmogorov 1933). All the validations indicated that the estimation method developed herein provides acceptable estimates. A further validation in the future could include analyzing certified reference soil samples.

Uncertainty of the inverted concentrations was propagated from the uncertainty in the mineralogical data using the root-sum-squares (RSS) method following Ellison et al. (1997) and Taylor (2005). The resulting uncertainty on the SiO_2 estimates was found to be 14.1 wt%. In comparison, the uncertainty of the XRF-based SiO_2 quantification in the National Geochemical Survey of Australia is estimated at 7.3 wt% (three times the RSD of 0.04 x 61.06 wt% quoted in table 1 of Caritat and Cooper 2011b).

For brevity of this contribution, the reader is referred to the fuller version of this paper published in *Geochemistry: Exploration, Environment, Analysis* with a preprint available at https://doi.org/10.31223/X5C665 for details of the validation and uncertainty of the SiO_2 estimates.

FUTURE WORK

In a complementary approach in progress, we are developing a machine learning approach using linear regression and random forest algorithms to estimate SiO_2 where it is missing, based on geochemical information, mineralogical information, and both geochemical and mineralogical information. This method will be tested on various datasets, including the NASGL and Australian datasets, to ensure its universal applicability and will be reported separately (Grunsky et al. *in prep.*)

DATASETS

A worked example for the five selected samples of Figure 3 is available as a Microsoft Excel spreadsheet (NALG_Ch_oxides_with_estimated_SiO2_LOI_worked example.xlsx) at https://doi.org/10.5281/zenodo.8191288. The new datasets including sample identification, coordinates, converted major oxide concentrations, and the concentration estimates for SiO_2 and LOI in wt% for the A and C horizon datasets from the North American Soil Geochemical Landscapes (NASGL) project are available as comma-separated value files (NALG_Ah_oxides_with_estimated_SiO2_LOI.csv and NALG_Ch_oxides_with_estimated_SiO2_LOI.csv) at https://doi.org/10.5281/zenodo.8191288.

CONCLUSIONS

We provide a novel method for estimating the concentrations of silica (SiO_2 wt%) and loss-on-ignition (LOI wt%) in the North American Soil Geochemical Landscapes (NASGL) project datasets. These datasets include comprehensive elemental and mineralogical compositions, determined mostly by four-acid digestion Inductively Coupled Plasma (ICP) Atomic Emission Spectroscopy (AES) or Mass Spectrometry (MS), depending on the element, and Rietveld refinement X-Ray Diffraction (XRD), respectively. Unfortunately, neither Si/SiO_2 nor LOI are quantified, both of which are significant components of most soils. Our estimation method combines the precision of the ICP determinations with the completeness of the XRD data. As the NASGL samples contain up to 95 wt% amorphous material of unknown geochemical or mineralogical composition, it is not

continued on page 13

Inverting the missing SiO_2 and LOI contents ...

continued from page 12

possible to directly calculate SiO_2 or LOI contents from mineralogy alone. However, a recursive inversion approach, i.e., calculating geochemistry from mineralogy, can be invoked to calculate minimum SiO_2, H_2O and CO_2 concentrations. Thus, we inverted an estimate for SiO_2 by adding up the SiO_2 contributions from all Si-bearing minerals (silicates). This 'normative' SiO_2 represents a minimum estimation of the total SiO_2 in each sample. Similarly, we inverted estimates for H_2O by adding up the H_2O contributions from all O-H-bearing minerals (hydrates), and for CO_2 by adding up the CO_2 contributions from all C-bearing minerals (carbonates). Combining the latter two components gives a minimum estimate for LOI. Thus, **100 wt% - (all major oxides from ICP + TEs from ICP + 'normative' H_2O + 'normative' CO_2)**, yields a maximum estimate of the total SiO_2 in each sample. The final or 'consensus' SiO_2 estimate is then calculated as the average between the two aforementioned estimates, trimmed as necessary to yield a total composition (**all major oxides from ICP + estimated SiO_2 + TEs from ICP + 'normative' H_2O + 'normative' CO_2**) of no more than 100 wt%. For most samples, the above sum falls below 100 wt% and the difference is taken to represent LOI not otherwise accounted for in the quantified hydrate and carbonate minerals. The source of this LOI contribution likely includes H_2O and CO_2 in the amorphous phase as well as other volatile components present in soil. We examine the statistical distributions of the SiO_2 and LOI estimates and validate the technique against a separate dataset from Australia where XRF, ICP and XRD data on the same samples exist. The correlation between predicted and observed SiO_2 is deemed strong ($R^2 = 0.91$). Further, we compared the estimated NASGL C horizon SiO_2 estimates with an independent dataset covering the conterminous USA, the 'Shacklette and Boerngen' dataset. The distributions of these two datasets are shown by a Kolmogorov-Smirnov test to be statistically identical. Spatially we demonstrate that the closest NAGSL sites and 'Shacklette and Boerngen' sites have highly correlated SiO_2 concentrations ($R^2 = 0.79$). Together, these validation assessments give us the confidence to recommend the approach of combining geochemical and mineralogical datasets to estimate missing SiO_2 and LOI in datasets elsewhere. However, as each situation is different, any estimation results ideally should be ground-truthed.

The full paper of this article is published in Geochemistry: Exploration, Environment, Analysis and is available at https://doi.org/10.1144/geochem2023-039.

ACKNOWLEDGMENTS

We appreciate comments on a draft version of this manuscript by Laurel G. Woodruff (United States Geological Survey) as well as internal reviews by Philip Main and Tara Webster (Geoscience Australia). EXPLORE reviewer Alexandre Voinot and editor Beth McClenaghan are thanked for their comments. PdC publishes with permission from the Chief Executive Officer, Geoscience Australia.

REFERENCES

Achilles, C.N., Downs, G.W., Downs, R.T., Morris, R.V., Rampe, E.B., Ming, D.W., Chipera, S.J., Blake, D.F., Vaniman, D.T., Bristow, T.F., Yen, A.S., Morrison, S.M., Treiman, A.H., Craig, P.I., Hazen, R.M., Tu, V.M. and Castle, N. 2018. Amorphous phase characterization through X-ray diffraction profile modeling: implications for amorphous phases in Gale Crater rocks and soils. 49th Lunar and Planetary Science Conference, LPI Contribution 2083, 2661. https://www.hou.usra.edu/meetings/lpsc2018/pdf/2661.pdf

Aitchison, J., 1986. The Statistical Analysis of Compositional Data. Chapman and Hall, London, 416 p. ISBN 9781930665781.

Aldis, M., Posch, M. and Aherne, J. 2023. Normative mineralogy of 1170 soil profiles across Canada. Minerals, 13, 544. https://doi.org/10.3390/min13040544

Caritat, P. de and Cooper, M. 2011a. National Geochemical Survey of Australia: The Geochemical Atlas of Australia. Geoscience Australia, Record, 2011/20, 557 p. http://dx.doi.org/10.11636/Record.2011.020

Caritat, P. de and Cooper, M. 2011b. National Geochemical Survey of Australia: Data Quality Assessment. Geoscience Australia, Record, 2011/021, 478 p. https://pid.geoscience.gov.au/dataset/ga/71971

Caritat, P. de, Bloch, J. and Hutcheon, I. 1994. LPNORM: a linear programming normative analysis code. Computers & Geosciences, 20, 313–347. https://doi.org/10.1016/0098-3004(94)90045-0

continued on page 14

Inverting the missing SiO_2 and LOI contents ...

continued from page 13

Caritat, P. de, Petts, A. and Kelaart, C. 2023. Contribution towards a regolith mineralogy map of the Australian continent: A study in South Australia, Queensland and the Northern Territory. Geoscience Australia, Record, 2023/15. https://dx.doi.org/10.26186/147990

Chayes, F., 1960. On correlation between variables of constant sum. Journal of Geophysical Research, 65, 4185–4193. https://doi.org/10.1029/JZ065i012p04185

Deer, W.A., Howie, R.A. and Zussman, J. 2013. An Introduction to the Rock-Forming Minerals, 3rd edition. Mineralogical Society of Great Britain and Ireland, 498 p. ISBN 9780903056274.

Ellison, S., Wegscheider, W. and Williams, A. 1997. Measurement uncertainty. Analytical Chemistry, 69, 607A–613A. https://doi.org/10.1021/ac971793j

Finkl, C.W., 1981. Soil mineralogy. *In:* Mineralogy, Encyclopedia of Earth Science. Springer, Boston, MA. https://doi.org/10.1007/0-387-30720-6_133

Grunsky, E.C., Drew, L.J. and Smith, D.B. 2018. Analysis of the United States portion of the North American Soil Geochemical Landscapes Project – A compositional framework approach. *In:* Daya Sagar, B., Cheng, Q. & Agterberg, F. (eds), Handbook on Mathematical Geosciences, Springer, Cham, 313–346. ISBN 9783319789996. https://doi.org/10.1007/978-3-319-78999-6_17

Kolmogorov, A.N. 1933. Sulla determinazione empirica di una legge di distribuzione. Giornale dell'Istituto Italiano degli Attuari, 4, 83–91.

Palarea-Albaladejo, J., Martín-Fernández, J.A. and Buccianti, A. 2014. Compositional methods for estimating elemental concentrations below the limit of detection in practice using R. Journal of Geochemical Exploration, 141, 71–77. https://doi.org/10.1016/j.gexplo.2013.09.003

Scealy, J.L., Caritat, P. de, Grunsky, E.C., Tsagris, M.T. and Welsh, A.H. 2015. Robust principal component analysis for power transformed compositional data. Journal of the American Statistical Association, 110, 136–148. https://doi.org/10.1080/01621459.2014.990563

Schaetzl, R. and Anderson, S. 2007. Soils – Genesis and Geomorphology, 1st edition reprinted with corrections. Cambridge University Press, Cambridge, 817 p. ISBN 9780521812016.

Shacklette, H.T. and Boerngen, J.G. 1984. Element Concentrations in Soils and Other Surficial Materials of the Conterminous United States: An Account of the Concentrations of 50 Chemical Elements in Samples of Soils and Other Regoliths. United States Geological Survey, Professional Paper, 1270, 105 p. https://pubs.usgs.gov/pp/1270/

Smith, D.B. 2022. Geochemical and mineralogical soil survey of the conterminous USA: a project retrospective. Geochemistry: Exploration, Environment, Analysis, 22, geochem2022-031. https://doi.org/10.1144/geochem2022-031

Smith, D.B., Cannon, W.F., Woodruff, L.G. and Ellefsen, K.J., 2014. Geochemical and Mineralogical Maps for Soils of the Conterminous United States. United States Geological Survey, Open-File Report, 2014-1082, 386 p. https://doi.org/10.3133/ofr20141082

Smith, D.B., Cannon, W.F., Woodruff, L.G., Solano, Federico, Kilburn, J.E. and Fey, D.L. 2013. Geochemical and Mineralogical Data for Soils of the Conterminous United States. United States Geological Survey, Data Series, 801, 19 p. http://pubs.usgs.gov/ds/801

Smith, D.B., Solano, F., Woodruff, L.G., Cannon, W.F. and Ellefsen, K.J. 2019. Geochemical and Mineralogical Maps, with Interpretation, for Soils of the Conterminous United States. United States Geological Survey, Scientific Investigations Report, 2017-5118. https://pubs.usgs.gov/sir/2017/5118/index.html

Smith, R.J., Horgan, B., Rampe, E. and Dehouck, E. 2018. The composition of amorphous phases in soils and sediments on Earth and Mars. 49th Lunar and Planetary Science Conference, LPI Contribution 2083, 1779. https://www.hou.usra.edu/meetings/lpsc2018/pdf/1779.pdf

Tan, K.H., Perkins, H.F. and McCreery, R.A. 1970. The nature and composition of amorphous material and free oxides in some temperate regions and tropical soils. Communications in Soil Science and Plant Analysis, 1, 227–238. https://doi.org/10.1080/00103627009366262

Taylor, J.A. 2005. Uncertainty Analysis. ES 223: Rigid Body Dynamics-Fall 2004. Arkansas State University, Jonesboro, AR. Online Lecture Notes. http://myweb.astate.edu/sharan/PMC/LectureNotes/2006/Paper%20on%20Uncertainty%20Analysis.pdf

Tsukimura, K., Miyoshi, Y., Takagi, T., Suzuki, M. and Wada, S. 2021. Amorphous nanoparticles in clays, soils and marine sediments analyzed with a small angle X-ray scattering (SAXS) method. Scientific Reports, 11, 6997. https://doi.org/10.1038/s41598-021-86573-9

Tukey, J.W. 1977. Exploratory Data Analysis. Addison-Wesley Publishing Company, Reading, MA, 688 p. ISBN 9780201076165.